Fuzzy *C*-Means Image Segmentation Approach for Axle-Based Vehicle Classification

Zhuo Yao, Heng Wei, Zhixia Li, and Jonathan Corey

Vehicle classification information is vital to almost all types of transportation engineering and management applications, such as pavement design, signal timing, and safety. Although the vehicular length–based classification scheme is widely used by state departments of transportation, this scheme lacks the capability of accurately producing axle-based classification data. Limited by the capital cost, axle-based vehicle classification data sources are very narrow. This paper presents an image segmentation–based vehicle classification system with an attempt to increase the efficiency of axle-based vehicle classification. The video-based vehicle classification system Rapid Video-Based Vehicle Identification System (RVIS) is developed to identify the number of axles automatically from ground-truth videos. Through the testing of individual vehicle image data sets, it is shown that the RVIS system is capable of successfully detecting all FHWA 13 vehicle classes. However, larger-scale testing of the RVIS system with a predetermined set of morphological parameters produces less accurate results. Comparison of two testing hours shows that with greater effort in calibration, results can be improved significantly and a great potential for field application exists. The advantages of the RVIS system are its robust and fast algorithm and its flexibility in that it can be applied either from a mobile video source or at locations with traffic-monitoring videos available. The RVIS system is a proven vehicle classification data source that adds to other existing vehicle classification approaches.

Any state using traffic data for the allocation of federal funds is required to maintain a traffic-monitoring system that meets FHWA requirements. Many transportation agencies [i.e., state departments of transportation (DOTs) and metropolitan planning organizations] have recognized that traffic data support a growing variety of functions and critical decision-making processes. The need for data and the benefits that result from the required data must be balanced against available and potential resources to implement an effective and efficient traffic monitoring program. As part of a traffic-monitoring program, state DOTs are required to collect vehicle count, classification, weight, and speed data. Since participation in federally funded programs is essential to the integrity of a state's highway system, the accurate, efficient collection of traffic data becomes a critical component of transportation infrastructure management (*1*). The traffic data programs serve a variety of traffic engineering purposes, including planning, design, calibration, collection, distribution, analysis, reporting, and maintenance (*2*). The 2013 edition of the *Traffic Monitoring Guide* (*2*) defaults the application of the axle-based FHWA 13 scheme in the vehicle classification data format requirements. Common sources of axle-based vehicle classification data are intrusive in nature. They include pneumatic rubber tubes, piezoelectric sensors, and active infrared sensors. Pneumatic tube traffic counters usually provide the total number of axles at the end of a count, but an adjustment factor is usually required to convert the total number of axles to the total number of vehicles (*3*). The adjustment factor itself is usually an additional source of inaccuracy aside from the undercounting problem. A survey of state DOTs shows that the pneumatic rubber tube has been reported in regard to issues of data accuracy, weather interference, and limitations in lanes monitored (*4*). The piezoelectric sensor is capable of counting axles by sensing the passage of the vehicle's individual axles but may not be able to tell how many axles belong to one single vehicle. In practice, many of the automatic traffic recording stations use a piezo–loop–piezo (P-L-P) or loop–piezo–loop (L-P-L) configuration on the freeway for better performance. Comparative study results show that an active infrared device, such as the Infra-Red Traffic Logger, provides adequate accuracy for the FHWA axle-based classifications in comparison with other commercial products, such as radar detectors (*5*). Active infrared devices are, however, usually expensive to own, install, and maintain.

In recent years, video and image processing techniques have been shown to be cost-effective in various traffic data collection and traffic control applications (*6, 7*). Despite limits of dependence on lighting conditions, video-based systems have some advantages over intrusive axle-based vehicle methods; for example, low effect on the road infrastructure, low maintenance costs, robustness of feature detection from images, and ready availability from regional intelligent transportation systems centers. It is in the interests of state DOTs to check the performance periodically of available automatic traffic recording stations. However, it would be very labor-intensive and almost impossible to collect data manually for quality control at every desirable location. An efficient and fast method and associated tool for processing video to produce accurate traffic information are therefore needed to improve the quality and increase the sources for vehicle classification data acquisition. This paper hence presents an image segmentation approach to improve the accuracy of the axle-based vehicle classification.

Z. Yao, 735 ERC, and H. Wei and J. Corey, 792 Rhodes Hall, ART-Engines Transportation Research Laboratory, College of Engineering and Applied Science, University of Cincinnati, Cincinnati, OH 45221-0071. Z. Li, Department of Civil and Environmental Engineering, Speed School of Engineering, University of Louisville, W.S. Speed Building, Room 111, Louisville, KY 40292. Corresponding author: Z. Yao, yaozo@mail.uc.edu.

Transportation Research Record: Journal of the Transportation Research Board, No. 2595, Transportation Research Board, Washington, D.C., 2016, pp. 68–77.
DOI: 10.3141/2595-08

Yao et al. proposed a prototype of the Rapid Video-Based Vehicle Identification System (RVIS) with system function designs and preliminary results (*8*). This paper extends previous work on generating traffic classification data in three ways: (*a*) improving the previously developed computer vision-based algorithm to extract axle-based vehicle classification, (*b*) introducing the theoretical foundations of the proposed method, and (*c*) building the capability of automatically extracting traffic classification data from a larger video data set. The rest of the paper is organized as follows. The state-of-the-art computer vision applications in the traffic data extraction study are summarized as a result of the literature review, followed by a description of the method and data source used in this study. Case studies covering the FHWA Scheme F class vehicle results are then provided. Finally, a summary, conclusions, and recommendations for further research are presented.

SUMMARY OF EXISTING STUDIES

Much research has been conducted with data extracted from video- and image-based tools (*9–11*) at the University of Cincinnati. Zhang et al. used virtual dual-loop detectors set up in the video screen to mimic the functionality of dual-loop detectors (*12*). That approach filled the gap in traffic data extraction in cases in which dual-loop detectors were not available. However, the method is still model-based and has adapted the modeling errors pertaining in the system. Kanhere attempted to develop a video-based vehicle classification system with the use of pattern recognition (*13*). The method considered using wheels as a feature but did not provide reference to classification using the axle and its configuration. Hsieh et al. used size and linearity features to classify vehicles dynamically from a built library (*14*). This machine learning–based method is very dependent on library templates and usually requires a considerable amount of time and effort for the calibration process. Moreover, the classification has only four bins, representing a car, minivan, truck, and van truck, which may not satisfy the needs of the axle-based classification scheme. Ma and Grimson attempted to classify vehicles from edge points of a detected vehicle object from video (*15*). They used classification techniques to extract the vehicle shape. This effort is also library-based and requires a long time for learning and recognizing vehicles. Recently, Yao et al. developed a computer vision-based software tool, namely, the Rapid Traffic Emission and Energy Consumption Analysis (REMCAN) system (*16*). It enables rapid vehicle operating mode distribution profiling for the Motor Vehicle Emission Simulator (MOVES) model from video data. Clearly, the availability of ground-truth vehicle classification data will help to maximize the MOVES model capacity.

Less research effort has been reported involving the generation of axle-based vehicle classification data by using the recent development in computer vision and image-processing techniques. Frenzel proposed a video-based system in a heuristic study focused on truck detection and axle counting rather than vehicle classification (*17*). Results show only a 56% axle detection rate, which is a very low rate. Nevertheless, no vehicle classification study was carried out in this study. A couple of studies applied a three-dimensional (3-D) model–based computer vision system for vehicle classification (*18, 19*). The vehicles were modeled at the 3-D level and then categorized into classes. This method usually requires extensive expertise in computer vision techniques and computer programming, yet it produced misclassifications because one 3-D model may have multiple axle configurations according to FHWA Scheme F.

METHOD

The goal of this research was to explore an axle-based vehicle classification method with the use of existing image-processing techniques to fulfill the identified research gap. To achieve that goal, two objectives were chosen: (*a*) design a vehicle classification system, RVIS, based on vehicle axle numbers, and (*b*) test and validate the proposed axle parameter–based vehicle classification system with FHWA Scheme F classes. The proposed research addressed the challenges and identified the research gap through the development and testing of the proposed RVIS with a case study. The advantage of the proposed RVIS system is that it is a ground-truth video data–based, nonintrusive classification method. The ground-truth-based method is reliable since it bypasses the modeling and malfunctioning errors that conventional sensors might have. The video source is from a home entertainment grade camcorder that produces 1,024 × 768 videos at 30 frames/s.

Figure 1 shows the system flow of the RVIS. The RVIS system has four modules, namely, video to image, vehicle axle extraction, axle-based vehicle classification, and the calibration and validation module. The video-to-image module enhances, splits, and resizes raw video data into a series of images of individual vehicles with a common standard size. The vehicle axle extraction module is the core module in this system. It detects and segments the vehicle axle pixels with the fuzzy *C*-means clustering algorithm. The vehicle classification module, which contains predefined FHWA vehicle classification axle configurations, matches and classifies the outputs from the axle parameter extraction module. The classification is based on the number of axles. Finally, a calibration and validation module is designed to guarantee the performance of the proposed RVIS. This module uses the ground-truth video to check and correct any possible misclassifications and errors.

Background Segmentation and Foreground Extraction

A robust background subtraction algorithm should be able to handle lighting changes and long-term scene changes. To achieve this objective, the mean filter method was used. Let $V(x, y, t)$ represent a video sequence in which t is the time of the video frame and x and y are the two-dimension pixel location variables. To estimate the background image, a series of sequential frames were averaged in a sliding time window. The background image at time t was calculated as follows:

$$B(x, y) = \frac{1}{N}\sum_{i=1}^{N} V(x, y, t - i * m) \quad (1)$$

where

i = ith frame of the video sequence,
N = number of sequential images taken for averaging, and
m = number of consecutive frames between two neighboring sequential images.

N and m should be chosen carefully to capture an instant change in the environment, such as light change. After the background $B(x, y)$ has been estimated, the foreground at time t can be obtained by subtracting $B(x, y)$ from $V(x, y, t)$ and thresholding it. The foreground is

$$\left|V(x, y, t) - B(x, y)\right| = \text{Th} \quad (2)$$

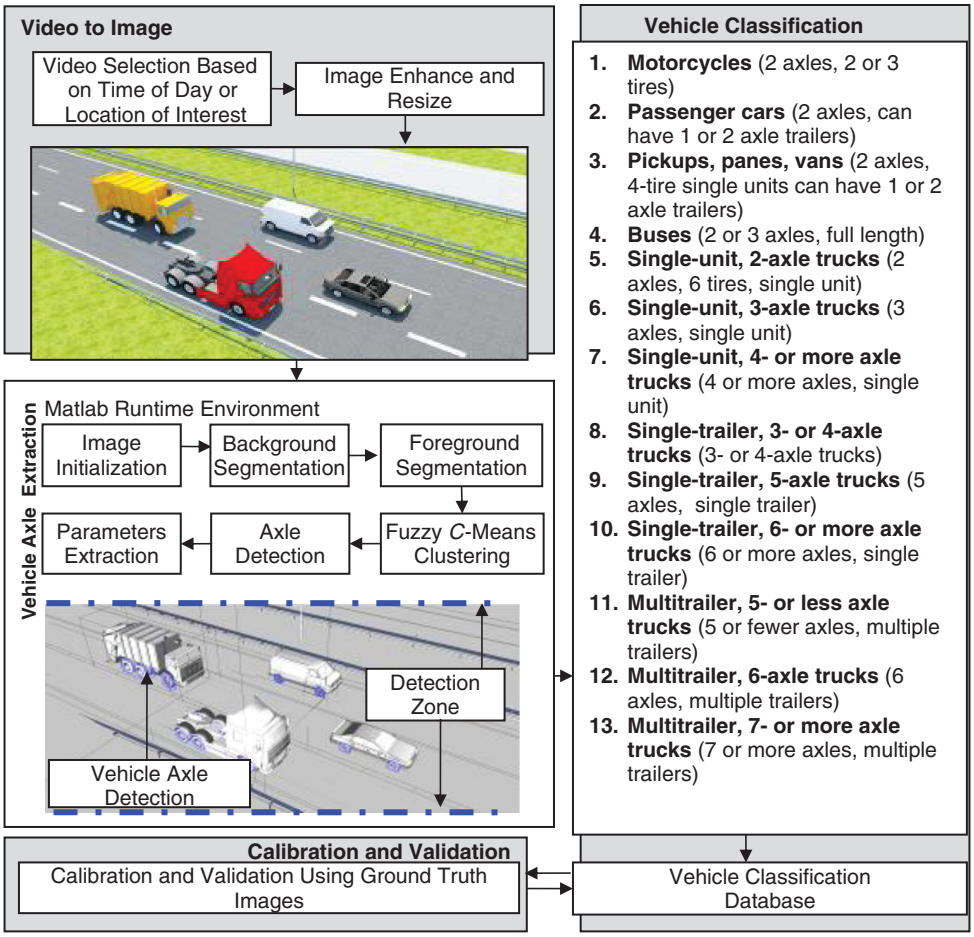

FIGURE 1 System flowchart for RVIS.

where Th is the threshold. The selection of Th would affect the accuracy of the foreground extraction. To remove noise in the foreground image, a set of morphological operations, including opening, closing, and dilation, were used in this project. Figure 2 further illustrates the background segmentation and foreground extraction process.

Fuzzy *C*-Means Clustering-Based Image Segmentation

Image segmentation is the process of segmenting a group of image pixels into a set of disjoint regions that have similar characteristics, such as intensity, color, and texture. A considerable number of image segmentation techniques are available. The clustering-based methods, which segment the feature space of the image into several clusters and derive a sketch of the original image, include *K*-means (*20*), fuzzy *C*-means (FCM) (*21, 22*), and mean-shift (*23*) algorithms. The FCM algorithm is widely applied to image segmentation because it has robust characteristics for ambiguity and the ability to retain much more information compared with threshold-based segmentation methods. FCM clustering is an unsupervised clustering technique applied to segment images into clusters with similar spectral properties. It uses the distance between pixels and cluster centers in the spectral domain to compute the membership function. The pixels in an image are highly correlated, and this spatial information is an important characteristic that can be used to develop the clustering. This technique was originally introduced by Bezdek in 1981 as an improvement on earlier clustering methods (*24*). It provides a method that shows how to group data points that populate some multidimensional space into a specific number of different clusters.

The FCM algorithm is an iterative optimization that minimizes the cost function J_{FCM}, defined as follows:

$$J_{FCM} = \sum_{k=1}^{K}\sum_{i=1}^{M\times N}\left|u_{ik}^{m}d_{ik}^{2}\right| = \sum_{k=1}^{K}\sum_{i=1}^{M\times N}u_{ik}^{m}\left\|x_i-\mu_k\right\|^2 \qquad 1\le m\le\infty \tag{3}$$

where

m = any real number greater than 1,
$M \times N$ = number of pixels in image,
u_{ik}^{m} = degree of membership of x_i in cluster k,
x_i = ith element of d-dimensional measured data,
μ_k = center of cluster with d-dimension (for images $d = 2$),
$d_{i,k}^{2}$ = distance measure between object x_i and cluster center μ_k, and
$||*||$ = any norm expressing similarity between any measured data and center μ_k.

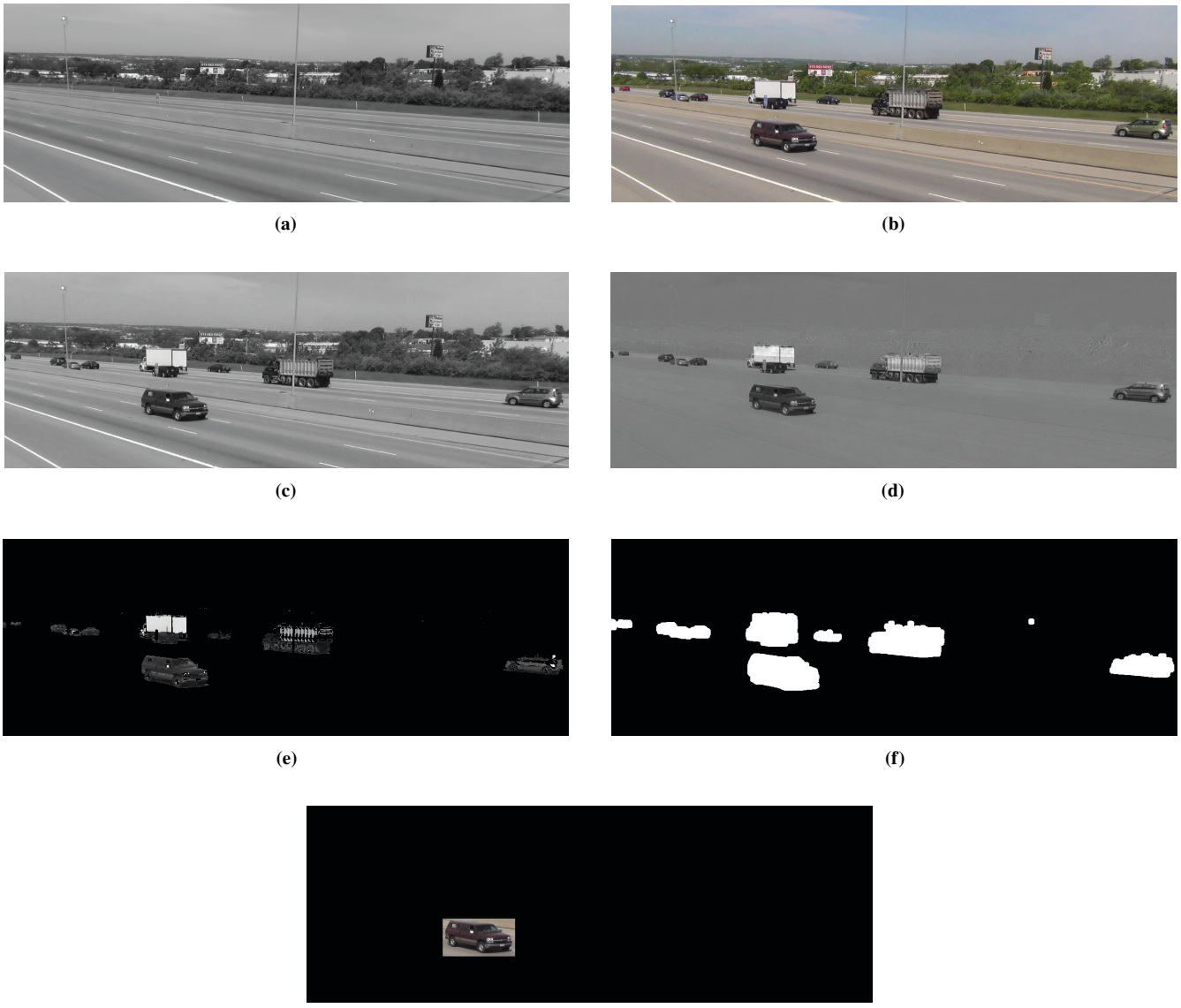

(a) **(b)** **(c)** **(d)** **(e)** **(f)** **(g)**

FIGURE 2 Sample background segmentation and foreground extraction: (*a*) Image 1, background; (*b*) Image 2, new video frame; (*c*) Image 3, grayscale new video frame; (*d*) Image 3 subtracts (digital numeric value of whole image subtracted from another image) from Image 1; (*e*) Image 5, resulting image after black and white thresholding; (*f*) Image 6, binary image of Image 5; and (*g*) Image 7, segmented foreground image by multiplying Image 6 by Image 2.

The cost function is achieved when pixels with a short distance to the centroid of their clusters are assigned with high membership values while pixels far from the centroid are assigned to low membership values. The membership function represents the probability (fuzziness) that a pixel belongs to a specific cluster to some degree. The probability is dependent solely on the distance between the pixel and each individual cluster center in the feature domain.

Fuzzy partitioning is carried out through an iterative optimization of the objective function shown previously, with the update of membership u_{ik} and the cluster centers μ_k by

$$u_{ik} = \frac{1}{\sum_{i=1}^{K} \left(\frac{d_{ik}}{d_{ij}} \right)^{-\frac{2}{m-1}}} \tag{4}$$

$$\mu_k = \frac{\sum_{i=1}^{MN} u_{ik^m} x_i}{\sum_{i=1}^{MN} u_{ik^m}} \tag{5}$$

This iteration stops when

$$\max_{ik} \left\{ \left| u_{ik}^{(n+1)} - u_{ij}^{(n)} \right| \right\} < \varepsilon$$

where

ε = termination criterion between 0 and 1,
d_j = jth of the d-dimensional measured data, and
n = number of iterations.

This procedure converges to a local minimum or a saddle point of error.

The FCM algorithm is applied directly on the pixels of an image. The degree of membership of pixels in each class is therefore calculated. Starting with an initial guess at each cluster center, FCM converges on a solution for μ_k representing the local minimum or a saddle point of the cost function. Convergence can be detected by comparing the changes in the membership function or the cluster center of two successive iteration steps.

The algorithm is composed of the following steps (*25*):

Step 1. Set values for *M, N, m,* and ε.
Step 2. Initialize $U = [u_{ik}]$ matrix, $U^{(0)}$.
Step 3. Set the loop counter $b = 0$.
Step 4. At *n*-step: calculate the center vectors $\mu^{(n)} = [\mu_k]$ with $U^{(n)}$.

$$\mu_k = \frac{\sum_{i=1}^{MN} u_{ik^m} x_i}{\sum_{i=1}^{MN} u_{ik^m}} \tag{6}$$

Step 5. Update $U(n)$, $U(n+1)$.

$$u_{ik} = \frac{1}{\sum_{i=1}^{K} \left(\frac{d_{ik}}{d_{ij}} \right)^{\frac{2}{m-1}}} \tag{7}$$

Step 6. If $||U(n+1) - U(n)|| < \varepsilon$, then STOP; otherwise set $b = b + 1$, and return to Step 4.

In each iteration of the algorithm, $M \times N \times k$ probability functions are calculated (k is the number of classes). Figure 3 shows an illustration of the FCM clustering results. In this case, the pixels composing the vehicle tires are highlighted in the crosshair (Figure 3*a*) and clustered into a group as shown in the red, green, blue (RGB) color space (Figure 3*b*). The tire pixels have an average RGB value of 58, 58, 58 (grayish tire colors tend to have similar RGB values) and share 4.23% of the total number of pixels in the image.

Axle Detection

The axle parameter extraction module fine-tunes the axle segmentation and is illustrated with an example in Figure 4. This module takes in an input image and begins with FCM clustering to segment out the tires from the image (Figure 4*b*). Then, the color information of the image can be discarded, and it is converted into a grayscale image (Figure 4*c*). Figure 4*d* shows the result of morphological opening (filtering out the small objects in the image) on the grayscale or binary image with the structuring element. The morphological open operations, erosion followed by dilation, use the same structuring element for both operations. After this, a hole-filling process is performed in which a hole is defined as a set of background pixels that cannot be reached by filling in the background from the edge of the image (Figure 4*e*). The difference between Figure 4*e* and Figure 4*d* (mathematical operation), which represents the wheel entity, is shown in Figure 4*f*. The final step (Figure 4*g*) simply extracts the segmented wheels' parameter. Further axle-based classification will be performed on the basis of results from this step.

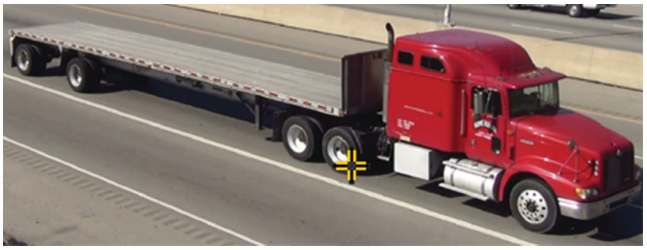

(a)

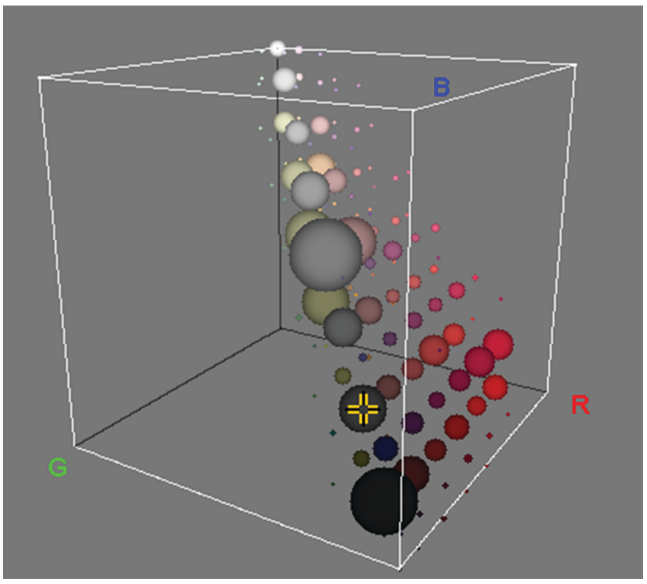

(b)

FIGURE 3 FCM clustering on axle pixels (RGB: 58, 58, 58; percentage = 4.23%): (*a*) original image with marked tire pixels and (*b*) classified tire pixel cluster based on RGB value.

To reduce noise further and extract vehicle tires, two morphological operators are used: erosion and dilation. If a foreground object has some holes in it, the application of these two operators will fill the holes. If small foregrounds that were not connected to a big foreground object are detected, they will be eliminated.

Erosion in a binary image can be expressed as

$$A \ominus B = \bigcap_{b \in B} A_b$$

where A is a binary image. In a binary image, 1 represents white and 0 represents black. B is a 3×3 matrix with a center anchor (with each element having a value of one) and is convolved with the entire image. Figure 5 shows the result of this operation on a binary image. It can be seen that this operator was able to eliminate the noisy and unwanted objects.

Dilation can be expressed as

$$A \oplus B = \bigcup_{b \in B} A_b$$

Figure 6 shows the result of this operation on a binary image. It can be seen that this operator was able to connect the relevant parts.

(a)

(b)

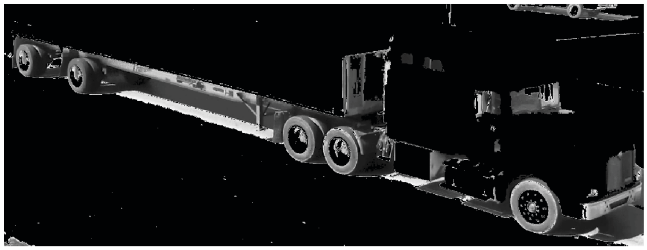

(c)

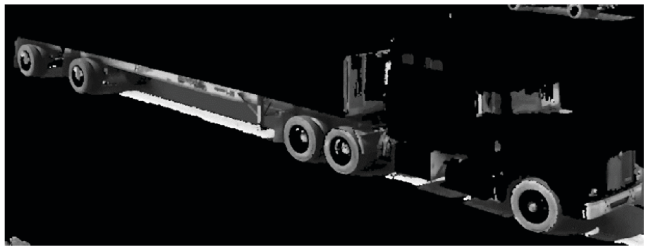

(d)

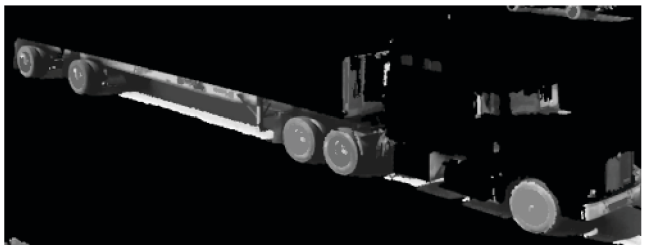

(e)

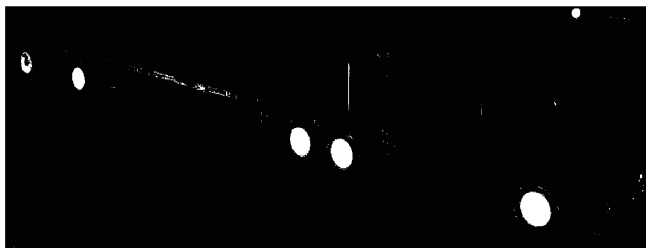

(f)

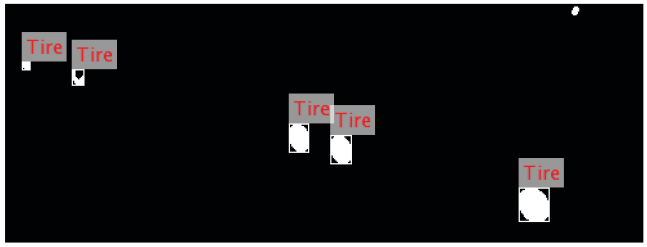

(g)

FIGURE 4 Axle detection and extraction process: (*a*) Image 1, input; (*b*) Image 2, fuzzy *C*-means clustering; (*c*) Image 3, convert image to grayscale; (*d*) Image 4, filter out small objects (binary large object); (*e*) Image 5, fill out closed areas in image; (*f*) Image 6, subtract Images 5 and 4 and then convert to binary image; and (*g*) Image 7, feature detection and extraction.

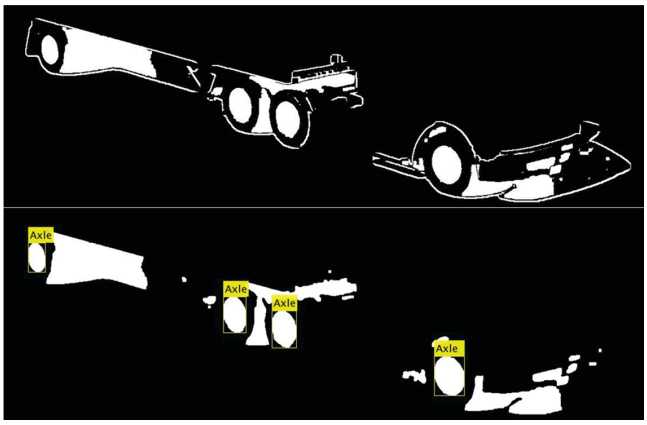

FIGURE 5 Result of erosion operator on binary image.

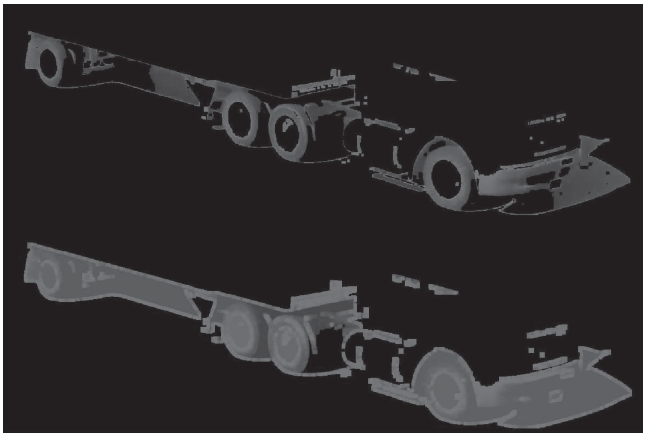

FIGURE 6 Result of dilation on binary image.

This technique is used after the FCM image pixel classification. It has a significant effect on accuracy because it identifies the axles.

RESULTS

The RVIS case study used video data collected on October 19, 2013, at I-275 Mile Marker 45–46, in Cincinnati, Ohio. The case study results focused on covering the full spectrum of the 13 FHWA classes rather than single or several classes. A selection of FHWA 13 class vehicle images from the RVIS video-to-image module is used to test the FCM clustering algorithm. Figure 4 shows the axle detection and parameter extraction results with the FHWA 13 vehicle classification scheme. The first image line shows the original images as input for the RVIS. The second image line shows the result using FCM segmented axles. The third image line shows the hole filling result from the rim of the axle. The binary images show the difference between the holes-filled image and the segmented image. The last image in Figure 4 shows the axle blobs where the number of axles is identified.

For Class 1 vehicles (i.e., motorcycles) and Class 4 vehicles (i.e., buses), the RVIS methods used were not axle-based. For Class 1 motorcycles, all the rear axles of the motorcycles are covered and it is impossible for the program to segment them out. Therefore, in the case study below, Class 1 vehicles are detected only as vehicles with one axle. For Class 4 vehicles, the sample is an image of a yellow school bus (there are no other types of buses running on the stretch of freeway in the data collection). It is simpler to detect the color yellow just by its RGB values at the 255, 255, 0 range. This approach is a faster and more efficient way to determine the vehicle class if the vehicle is a yellow school bus.

Figure 7 shows the successful result of the RVIS detection of the axle-based FHWA 13 classes. The large-scale, automatic running of 2 h of video data is presented in Table 1. After the video data were processed, the results were compared with the ground-truth images extracted from the video data set by the RVIS.

Table 1 summarizes the RVIS results after a 2-h test was conducted. Because vehicles with a higher number of axles are on the road less, the sample size distribution is extremely loaded toward two-axle vehicles. The RVIS was able to sample out 1,397 vehicles from the video data and generated 842 correctly identified vehicles for the first hour. The detection rate was 60.27%. For the second hour, the sample size was 1,300, with 803 correctly identified. The detection rate here was 65.31%. After the 2 h of RVIS detection were averaged, the overall detection rate was 62.79%. The morphological operators (erosion and dilation) for Hour 1 and Hour 2 are calibrated to improve the detection rate. Table 1 results show that RVIS accuracy can be improved when the morphological operators are better calibrated to adapt to changes in the lighting environment.

Although the relative detection rate is approximately 63%, the RVIS system still has some advantages compared with other automated vehicle classification methods. First, the RVIS is inexpensive to deploy, run, and generate results because it bypasses the intrusive nature of traditional automated vehicle classification methods, such as the use of loop detectors. The RVIS could be deployed easily at any desired location that is in need of vehicle classification data with just a home camcorder. Since it is so easy to deploy video cameras and record the video data, the RVIS can potentially cover a much larger spatial territory without an investment in automatic vehicle classification devices. In addition, the RVIS could provide data at locations such as truck terminals, bus terminals, air ports, and logistic centers, to generate axle-based vehicle classification

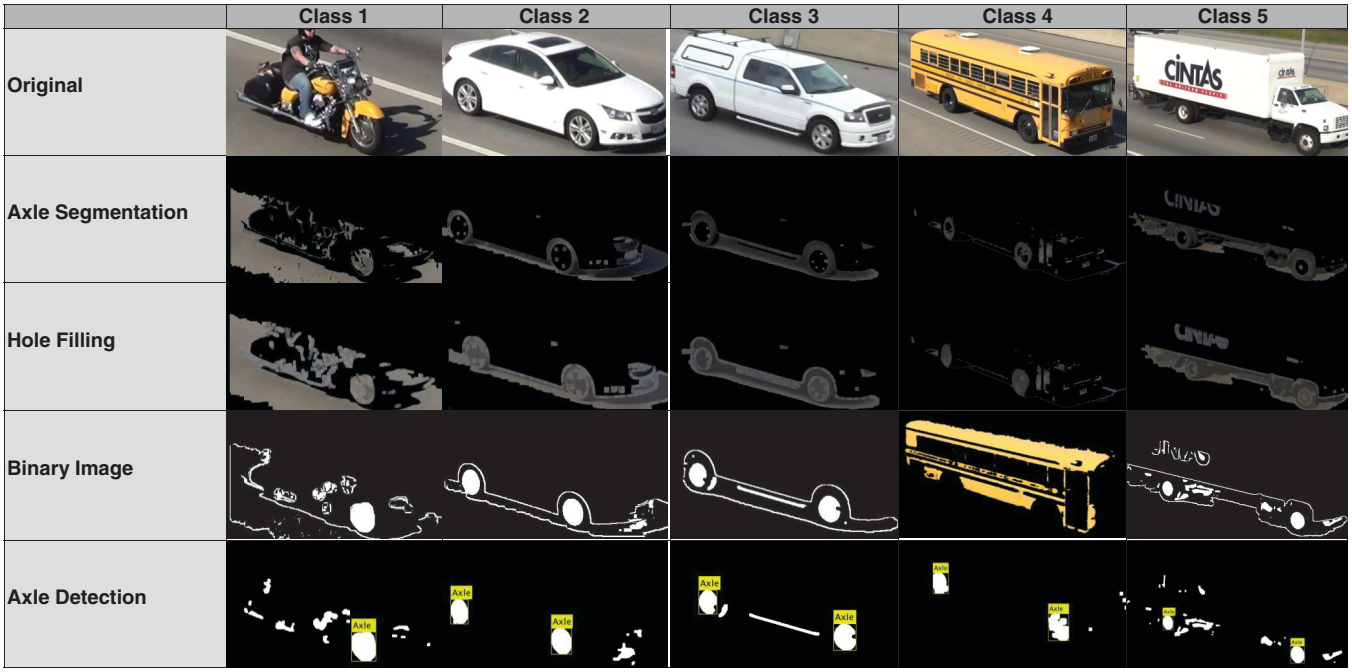

(a)

FIGURE 7 Axle detection results for FHWA 13 classes: (*a*) images for Classes 1–5.
(continued)

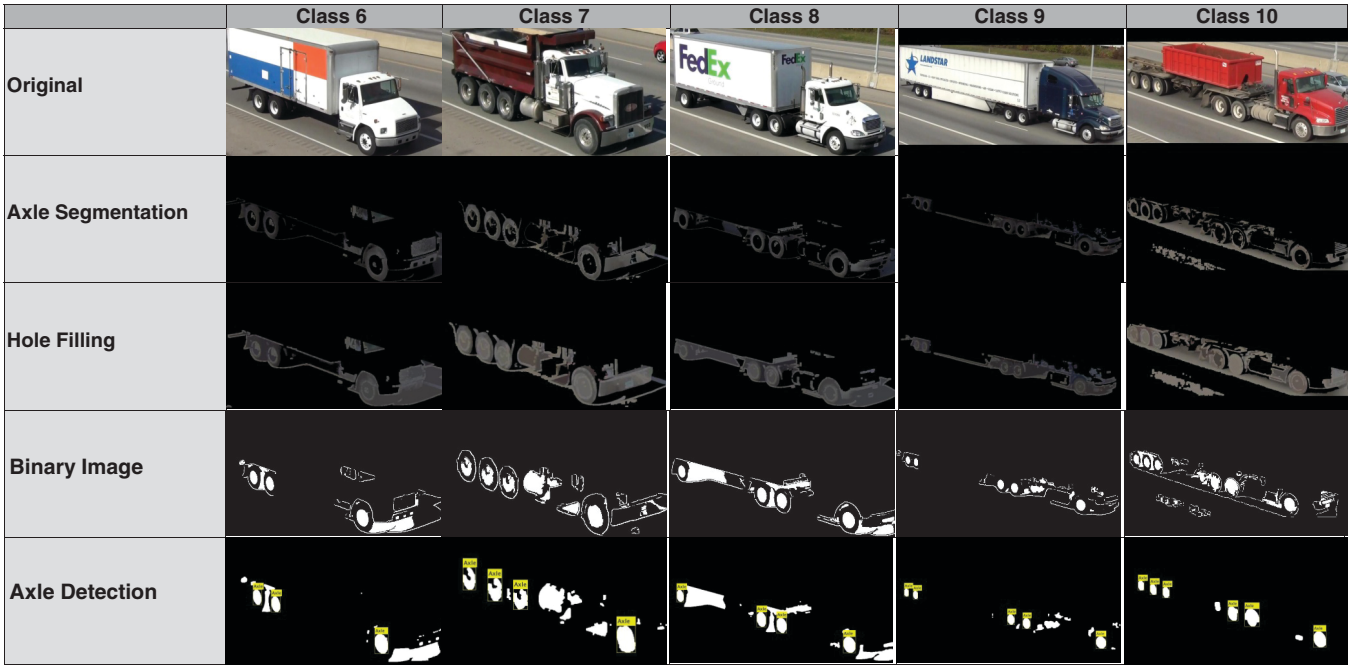

(b)

(c)

FIGURE 7 *(continued)* Axle detection results for FHWA 13 classes: (*b*) images for Classes 6–10 and (*c*) images for Classes 11–13.

TABLE 1 RVIS Detection Rate Summary

	Detection Results by Hour					
	Hour 1			Hour 2		
Vehicle Axle Type	Ground Truth (number of vehicles)	RVIS Result (number of vehicles)	Detection Rate (%)	Ground Truth (number of vehicles)	RVIS Result (number of vehicles)	Detection Rate (%)
2-axle	1,322	813	61.50	1,228	759	61.81
3-axle	9	1	11.11	12	8	66.67
4-axle	8	2	25.00	7	1	57.14
5-axle	52	24	46.15	51	14	54.90
6-axle	5	1	20.00	2	1	50.00
7-axle	1	1	100.00	3	1	66.67
School bus	—	—	—	1	1	100.00
Detection results by hour	1,397	842	60.27	1,300	803	65.31

NOTE: — = no data available. Overall detection rate = 62.79%.

data for the purposes of freight modeling, travel demand model calibration and validation, and safety studies, among others. This ability alone saves capital and time and avoids the safety risks of installing the intrusive devices. Nevertheless, the RVIS could generate data when a traditional data collection method fails in conditions such as congestion. Under conditions such as congestion, since the traffic was moving very slowly or not at all, errors were introduced into data collection methods such as loop detectors. The RVIS, however, could capture the true vehicle axles since it is ground truth–based rather than modeled algorithm–based.

CONCLUSION

This research sets out an alternative vehicle classification data source enabling low-cost performance compared with that of traditional data sources such as automatic traffic recording stations. The RVIS system helps transportation agencies' traffic data programs to achieve accurate vehicle classification data, which are critical to transportation engineering, safety, and management applications. The proposed vehicle classification approach makes the following contributions to currently used vehicle classification data collection: the approach (*a*) provides a low-cost way of collecting vehicle classification data that can diagnose performance over existing data sources such as loop detectors and radar; (*b*) provides an alternative vehicle classification data source when a traditional classification method fails; and (*c*) complements the existing vehicle classification data sources spatially and temporally. Preliminary results showed that the RVIS is capable of providing vehicle classification information and is potentially capable of providing supportive grounds for decision makers to confront the challenge of investing wisely in rehabilitation, maintenance, materials, and processes. The low-cost vehicle classification method will expand the vehicle classification data coverage and performance and will return cheaper and more location-available results.

The case study testing the FHWA 13 classes of vehicles shows that the RVIS system can be an additional vehicle classification data source on top of existing vehicle classification data collection methods. Although results are preliminary, the RVIS system is indeed capable of accurately detecting all FHWA 13 vehicle classes from the testing images, as shown in Figure 7. Large-scale testing of RVIS running with a set of morphological parameters produces more accurate results and should be performed. However, the second hour produced higher accuracy with a better set of calibrated morphological parameters. Comparison of the two testing hours shows that with a greater calibration effort, results can be improved. The advantages of the RVIS are its robust and fast algorithm and its flexibility to be applied either at a mobile video source or at locations where traffic-monitoring videos are available. Therefore, RVIS expanded the availability of the vehicle classification data locations in the roadway network. Future work includes continuously improving the algorithm in detection to adapt to changes in the lighting environment, developing a calibration protocol to produce more accurate results, testing with larger data sets, and improving the performance of the RVIS system as evaluated against other automated vehicle classification methods. Issues related to low lighting or lighting environment changes should also be explored with the use of alternative video sources such as thermal videos. Since all video-based data collection systems are "what you see is what you get" types of applications, another potential improvement is to solve the vehicle occlusion issues. In addition, a thorough analysis of the economic benefit and cost of the proposed RVIS system in comparison with other types of automated vehicle classification methods would be beneficial.

REFERENCES

1. Jeng, S.T., and S.G. Ritchie. Real-Time Vehicle Classification Using Inductive Loop Signature Data. In *Transportation Research Record: Journal of the Transportation Research Board, No. 2086,* Transportation Research Board of the National Academies, Washington, D.C., 2008, pp. 8–22.
2. *Traffic Monitoring Guide.* FHWA, U.S. Department of Transportation, 2013.
3. Hallenbeck, M., and H. Weinblatt. *NCHRP Report 509: Equipment for Collecting Traffic Load Data.* Transportation Research Board of the National Academies, Washington, D.C., 2004.
4. Skszek, S. *State-of-the-Art Report on Non-Traditional Traffic Counting Methods.* Arizona Department of Transportation, Phoenix, 2001.
5. Yu, X., P.D. Prevedouros, and G. Sulijoadikusumo. Evaluation of Autoscope, SmartSensor HD, and Infra-Red Traffic Logger for Vehicle Classification. In *Transportation Research Record: Journal of the Transportation Research Board, No. 2160,* Transportation Research Board of the National Academies, Washington, D.C., 2009, pp. 77–86.

6. Kastrinaki, V., M. Zervakis, and K. Kalaitzakis. A Survey of Video Processing Techniques for Traffic Applications. *Image Vision Computation,* Vol. 21, No. 4, 2003, pp. 359–381.
7. Foresti, G., C. Micheloni, and L. Snidaro. Advanced Visual-based Traffic Monitoring Systems for Increasing Safety in Road Transportation. *International Journal of Advanced Transportation Studies,* Vol. 1, No. 1, 2003, pp. 27–47.
8. Yao, Z., H. Wei, X. Xiao, H. Liu, and H. Ren. Prototype of Video-Based Vehicle Classification System Using Vision-Based Axle Detection. Presented at 93rd Annual Meeting of the Transportation Research Board, Washington, D.C., 2014.
9. Wei, H., E. Meyer, J. Lee, and C. Feng. Video-Capture-Based Approach to Extract Multiple Vehicular Trajectory Data for Traffic Modeling. *ASCE Journal of Transportation Engineering,* Vol. 131, No. 7, 2005, pp. 496–505.
10. Wei, H. *Characterize Dynamic Dilemma Zone and Minimize Its Effect at Signalized Intersections.* 2008 Ohio Transportation Consortium Project Report, University of Akron, Ohio, 2008.
11. Wei, H., Z. Li, and Q. Ai. Observation-based Study of Intersection Dilemma Zone Natures. *Journal of Safety and Security,* Vol. 1, No. 4, 2009, pp. 282–295.
12. Zhang, G., R.P. Avery, and Y. Wang. Video-Based Vehicle Detection and Classification System for Real-Time Traffic Data Collection Using Uncalibrated Video Cameras. In *Transportation Research Record: Journal of the Transportation Research Board, No. 1993,* Transportation Research Board of the National Academies, Washington, D.C., 2007, pp. 138–147.
13. Kanhere, N. *Vision-Based Detection, Tracking and Classification of Vehicles Using Stable Features with Automatic Camera Calibration.* PhD dissertation. Clemson University, Clemson, S.C., 2008.
14. Hsieh, J., S. Yu, Y. Chen, and W. Hu. Automatic Traffic Surveillance System for Vehicle Tracking and Classification. *IEEE Transactions on Intelligent Transportation Systems,* Vol. 7, No. 2, 2006, pp. 175–187.
15. Ma, X., and W. Grimson. Edge-Based Rich Representation for Vehicle Classification. *Tenth IEEE International Conference on Computer Vision,* Vol. 2, 2005, pp. 1185–1192.
16. Yao, Z., H. Wei, Z. Li, T. Ma, and H. Liu. Developing Operating Mode Distribution Inputs for MOVES Using Computer Vision-Based Vehicle Data Collector. In *Transportation Research Record: Journal of the Transportation Research Board, No. 2340,* Transportation Research Board of the National Academies, Washington, D.C., 2013, pp. 49–58.
17. Frenzel, J. *A Video-Based Method for the Detection of Truck Axles.* Idaho Department of Transportation, Boise, 2002.
18. Messelodi, S., C.M. Modena, and M. Zanin. A Computer Vision System for the Detection and Classification of Vehicles at Urban Road Intersections. *Pattern Analysis and Applications,* Vol. 8, No. 1/2, Sept. 2005, pp. 17–31.
19. Buch, N., M. Cracknell, J. Orwell, and S. Velastin. Vehicle Localisation and Classification in Urban CCTV Streams. In *Proceedings of 16th ITS World Congress,* 2009, pp. 1–8.
20. Papamichail, G., and D. Papamichail. The K-Means Range Algorithm for Personalized Data Clustering in e-Commerce. *European Journal of Operational Research,* Vol. 177, No. 3, 2007, pp. 1400–1408.
21. de Carvalho, F. Fuzzy C-Means Clustering Methods for Symbolic Interval Data. *Pattern Recognition Letters,* Vol. 28, No. 4, March 2007, pp. 423–437.
22. Clausi, D. K-Means Iterative Fisher (KIF) Unsupervised Clustering Algorithm Applied to Image Texture Segmentation. *Pattern Recognition,* Vol. 35, No. 9, Sept. 2002, pp. 1959–1972.
23. Comaniciu, D., and P. Meer. Mean Shift: A Robust Approach Toward Feature Space Analysis. *IEEE Transactions on Pattern Analysis and Machine Intelligence,* Vol. 24, No. 5, Aug. 2002, pp. 603–619.
24. Bezdek, J., R. Ehrlich, and W. Full. FCM: The Fuzzy C-Means Clustering Algorithm. *Computers and Geosciences,* Vol. 10, No. 2/3, 1984, pp. 191–203.
25. Chuang, K.S., H.-L. Tzeng, S. Chen, J. Wu, and T.J. Chen. Fuzzy C-Means Clustering with Spatial Information for Image Segmentation. *Computerized Medical Imaging and Graphics,* Vol. 30, No. 1, Jan. 2006, pp. 9–15.

The Standing Committee on Artificial Intelligence and Advanced Computing Applications peer-reviewed this paper.